molecular pharmaceutics

ARTICLE

pubs.acs.org/molecularpharmaceutics

Novel Tetrapeptide, RGDF, Mediated Tumor Specific Liposomal Doxorubicin (DOX) Preparations

Huirui Du,[†,‡] Chunying Cui,[†,‡] Lili Wang,[§] Hu Liu,[*,§] and Guohui Cui[*,†]

[†]School of Chemical Biology and Pharmaceutical Sciences, Capital Medical University, Beijing, China. 100069

[§]School of Pharmacy, Memorial University of Newfoundland, St. John's, NL, Canada A1B 3V6

Supporting Information

ABSTRACT: Arginine-glycine-aspartate (RGD) has been shown to possess a strong affinity for the integrins overexpressed in tumor cells, especially during tumor invasion, angiogenesis and metasis. Based on work from others, a novel tetrapeptide, arginine-glycine-aspartate-phenylanaline (RGDF), has been designed and studied as a homing device to direct liposomal doxorubicin (DOX) to tumor cells in this work. In order to incorporate RGDF into liposomal DOX preparations, RGDF was conjugated with three different fatty alcohols to achieve RGDF−fatty alcohol conjugates. Glycine-glycine-aspartate-phenylanaline (GGDF)-lauryl alcohol conjugate was synthesized as a negative control. RGDF−fatty alcohol conjugates (RGDFO$(CH_2)_nCH_3$) and GGDF−lauryl alcohol conjugate (L-GGDFC12-DOX) incorporated liposomal preparations were obtained by first preparing liposomes using the film dispersion method followed by loading DOX using a transmembrane pH gradient method. Because of their amphipathic nature, RGDF− or GGDF−fatty alcohol conjugates are expected to be readily incorporated into liposomes with their fatty alkanyl chains being intercalated between fatty acyl chains of liposomal bilayers and the hydrophilic peptide moiety (RGDF or GGDF) being anchored on the surface of liposomes. The particle size and zeta potential of liposomal DOX preparations containing RGDF−fatty alcohol conjugate (L-RGDF-DOXs) or L-GGDFC12-DOX were measured, and their morphology was studied using transmission electron microscopy. *In vitro* DOX release profile from RGDF incorporated liposomal DOX was measured. The antitumor activities of RGDF incorporated liposomal DOX preparations were evaluated in ICR mice inoculated with sarcoma S_{180}, which is known to express $\alpha_v\beta_3$ integrin. Both conventional liposomal DOX preparation (L-DOX) without RGDFO$(CH_2)_nCH_3$ and L-GGDFC12-DOX were used as negative controls. Our results showed improved tumor growth inhibition with L-RGDF-DOXs over doxorubicin hydrochloride solution, L-DOX and L-GGDFC12-DOX. Pathological examination of tumor biopsy demonstrated that L-RGDF-DOXs induced enhanced tumor cell death in comparison to negative controls. Pharmacokinetic studies showed that the concentrations of DOX found in tumor sites were increased by 1.7−4.5-fold when liposomal DOX preparation containing RGDF−lauryl alcohol conjugate (L-RGDFC12-DOX) was administered in comparison to when L-GGDFC12-DOX or doxorubicin hydrochloride solution was administered. The concentrations of DOX found in the heart, which is the main site of toxic effects of DOX, were significantly reduced when L-RGDFC12-DOX was administered in comparison to when L-GGDFC12-DOX or doxorubicin hydrochloride solution was administered.

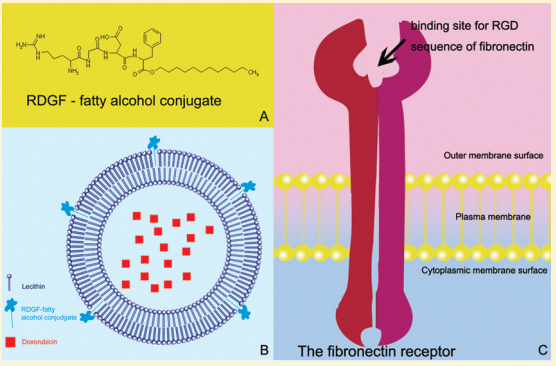

KEYWORDS: RGD, tumor specific liposomes, doxorubicin, antitumor, selective delivery of liposomes, drug targeting

1. INTRODUCTION

Doxorubicin (DOX) is a commonly used anticancer agent and belongs to anthracycline antibiotics. Like other anthracyclines, DOX is known to interact with DNA by intercalation and inhibition of DNA biosynthesis.[1] DOX inhibits the progression of the DNA topoisomerase II, which unwinds DNA for transcription. In addition, DOX stabilizes the topoisomerase II complex after the DNA chain has been broken for replication, preventing the DNA double helix from being resealed and thereby stopping the process of replication.[2] DOX is commonly used to treat certain types of leukemia, Hodgkin's lymphoma, and cancers of the bladder, breast, stomach, lung, ovaries, thyroid, soft tissue sarcoma, multiple myeloma, and others.[3] Major side effects of DOX include nausea, vomiting and heart arrhythmias. It also inhibits bone marrow functions causing neutropenia. Accumulative doses of DOX dramatically increase the risk of cardiac side effects, including congestive heart failure, dilated cardiomyopathy and death.[4−6]

Various targeted drug delivery strategies have been explored to improve the therapeutic index of anticancer agents. Liposomal systems of anticancer drugs have been marketed and shown to

Received: January 25, 2011
Accepted: June 1, 2011
Revised: April 26, 2011
Published: June 01, 2011

ACS Publications © 2011 American Chemical Society

have reduced toxicity.[7,8] However, better strategies are needed to improve the selectivity of existing systems. Immunoliposomes have been studied for active delivery of anticancer agents to tumors, in which tumor-specific antibodies are anchored on the surface of liposomal vesicles. After administration, they are expected to be actively associated with tumor specific antigens present on the surface of tumor cells. Therefore, anticancer agents encapsulated in such liposomes are expected to be actively delivered to tumor cells, resulting in reduced toxicity in normal cells.[9,10]

Integrins, a group of transmembrane proteins, are receptors that mediate an attachment between a cell and the tissues surrounding it, which may be other cells or the extracellular matrix. They are heterodimers containing two distinct chains, named α- and β-subunits,[11,12] and play an important role in tumor invasion and metastasis, a complex multistage process involving tumor−host interaction which includes adhesion, angiogenesis and proteolysis. Increased expression of integrins facilitates adhesion of tumor cells to the endothelial linings of blood vessels to colonize host organs.[13] It is known that the tripeptide arginine-glycine-asparate (Arg-Gly-Asp, RGD) has a strong affinity for integrins and demonstrated an inhibitory effect on the adhesion and angiogenesis of tumor cells.[14,15] RGD, however, also promotes the detachment of invasive tumor cells from the primary tumor site leading to the colonization of other organs.[16,17] Such dual and opposite effects on the progression of tumor limited the therapeutic potential of RGD in cancer treatment. Nevertheless, the elevated expression of integrins found in many tumors is well documented.[18,19] RGD has been conjugated to phospholipids and polyethylene glycols to achieve site specific liposomes.[20,21] However, studies so far involved complicated chemistry and unpredictable characteristics for formulations. In this work, a new tetrapeptide, arginine-glycine-aspartate-phenylalanine (Arg-Gly-Asp-Phe, RGDF), was designed to achieve improved affinity for integrins in tumor cells and to be used as a homing device on liposomes for targeting tumor cells. Phenylalanine, an aromatic amino acid, was added to RGD based on the findings from others that hydrophobic amino acids flanking the RGD motif increased binding affinity of RGD to integrins.[22,23] Liposomal DOX preparation was used to study the targeting potential of RGDF to tumor cells. In order to incorporate RGDF into liposomal DOX preparation to direct its delivery to tumor cells, RGDF−fatty alcohol conjugates ($RGDFO(CH_2)_nCH_3$) were designed as amphiphilic compounds (with both hydrophobic and hydrophilic characteristics) so that they would intercalate into the bilayers of liposomal DOX. Fatty alcohols of different chain lengths (C8, C12 and C16) were used in this work. Liposomal DOX preparations containing $RGDFO(CH_2)_nCH_3$ were prepared and evaluated. Glycine-glycine-aspartate-phenylanaline (GGDF) was synthesized as a negative control, in which arginine, a positively charged and bulky amino acid, found in RGDF was replaced by glycine, a neutral and much smaller amino acid. Mice inoculated with S_{180} sarcoma, which is known to express $\alpha_v\beta_3$ integrin, were used to examine the anticancer activity and targeting potential of the RGDF−fatty alcohol conjugate incorporated liposomal DOX preparations (L-RGDF-DOXs). Tissue distribution and pharmacokinetic profile of L-RGDF-DOXs in mice were also studied. The results were compared with those of conventional liposomal DOX preparation (L-DOX, containing no homing device) and GGDF−lauryl alcohol conjugate (L-GGDFC12-DOX) incorporated liposomal DOX preparation.

2. MATERIALS AND METHODS

2.1. Materials. Doxorubicin hydrochloride (pharmaceutical grade) was obtained from Beijing Huafeng United Technologies Ltd. (Beijing, China). Capryl alcohol (1-octanol, $CH_3(CH_2)_7-OH$), lauryl alcohol (1-decocanol, $CH_3(CH_2)_{11}-OH$) and cetyl alcohol (1-hexadecanol, palmityl alcohol, $CH_3(CH_2)_{15}-OH$) were obtained from Beijing Chaoyang Xudong Chemicals Inc. (Beijing, China). All amino acids and their protected forms were of L-configuration and were from Sichuan Sangao Biochemical Co. Ltd. (Chengdu, Sichuan, China). Dicyclohexylcarbodiimide (DCC), 1-hydroxybenzotriazole (HOBt), *N*-methylmorpholine (NMM), $BocArg(NO_2)OH$ and BocAsp(OBzl)OH were from GL Biochem Ltd. (Shanghai, China). Egg lecithin (MW = 750.00) was purchased from ACROS ORGANICS (Geel, Belgium). Cholesterol was purchased from Beijing Aoboxing Biotech Co. Ltd. (Beijing, China). All reagents were of chemical grade unless otherwise specified.

Animal experiments were carried out according to a protocol approved by the Experimental Animal Care Committee of Capital Medical University. Male Kunming and ICR mice purchased from the Animal Services, Capital Medical University were supplied with food and water *ad libitum*.

Laborota 4000 rotary evaporator was from Heidolph Instruments (Schwabach, Germany). An IKA.MS1 minishaker was purchased from Guangzhou, China. VCX500 ultrasonicator was a product of Sonics & Materials, Inc. (Newtown, CT, USA). Waters 2695 HPLC was used for quantitative analysis. An OLYMPUS IX71 inverted microscope equipped with a digital camera (OLYMPUS CAMEDIA C-7070) was purchased from Olympus Co. (Tokyo, Japan). A transmission electron microscope (TEM), JEM-1230, JEOL, was purchased from Japan. A particle size analyzer, Zetasizer Nano ZS-90, was purchased from Malvern Inc. (United Kingdom). A steam sterilizer was a product of VARIOKLAV (Germany).

2.2. Synthesis of $RGDFO(CH_2)_nCH_3$ and $GGDFO(CH_2)_{11}CH_3$. $RGDFO(CH_2)_nCH_3$ and $GGDFO(CH_2)_{11}CH_3$ were synthesized according to the schemes shown in Figures 1 and 2, respectively. The respective fatty alcohols of different carbon chain lengths (C8, C12 or C16) were first connected to the N-terminus protected phenylalanine (Boc-Phe-OH) in the presence of DCC, HOBt and NMM to yield N-terminus protected (Boc) phenylalanyl esters [$Boc\text{-}FO(CH_2)_nCH_3$, $n = 7$, 11 or 15]. After deprotection, $H_2N\text{-}FO(CH_2)_nCH_3$ ($n = 7$, 11 or 15) reacted with *N-tert*-butoxycarbonyl-L-aspartic acid 4-benzyl ester (Boc-Asp-OBzl) in the presence of DCC, HOBt and NMM to yield N-terminus protected 4-benzyl aspartylphenyalanyl esters, [$Boc\text{-}D(OBzl)FO(CH_2)_nCH_3$, $n = 7$, 11 or 15]. Protected dipeptides, arginine-glycine (RG) or glycine-glycine (GG), were formed by dissolving *N*-α-*tert*-butyloxycarbonyl-*N*-γ-nitro-L-arginine [$Boc\text{-}Arg(NO_2)\text{-}OH$] or *N-tert*-butoxycarbonyl-glycine (Boc-Gly-OH) and glycine benzyl ester tosylate (H-Gly-OBzl) in dimethylformamide (DMF). Condensation was completed in the presence of DCC and HOBt which resulted in $Boc\text{-}Arg(NO_2)\text{-}Gly\text{-}OBzl$ [$Boc\text{-}R(NO_2)G\text{-}OBzl$] or Boc-Gly-Gly-OBzl [Boc-GG-OBzl]. $Boc\text{-}R(NO_2)G\text{-}OBzl$ or Boc-GG-OBzl was then subjected to selective deprotection in the presence of 4 N NaOH (0 °C) to remove benzyl esters, which provided $Boc\text{-}R(NO_2)G\text{-}OH$ or Boc-GG-OH. Previously synthesized N-terminus protected 4-benzyl aspartylphenyalanyl esters [$Boc\text{-}D(OBzl)FO(CH_2)_nCH_3$, $n = 7$, 11 or 15] were subjected to treatment with 4 N HCl−EtAc to remove the N-terminus protection to yield 4-benzyl aspartylphenyalanyl esters [$H_2N\text{-}D(OBzl)FO(CH_2)_nCH_3$, $n = 7$, 11 or 15], which

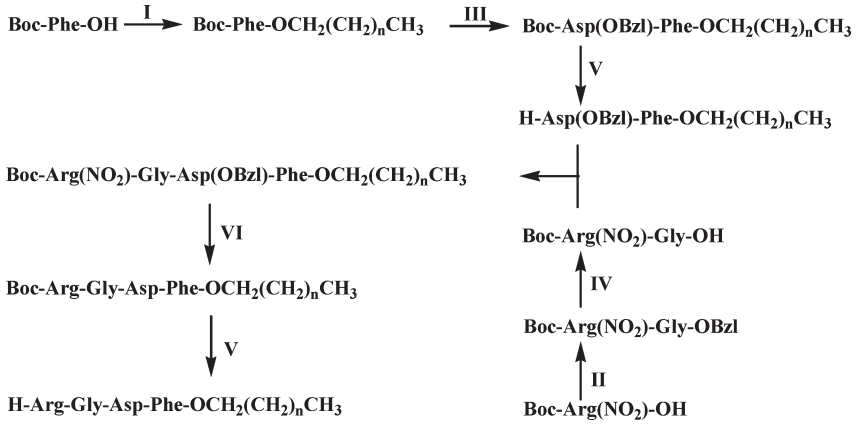

Figure 1. Synthesis of RGDFO$(CH_2)_nCH_3$ (n = 7, 11, 15): (I) DCC, HOBt, NMM and $CH_3(CH_2)_nOH$, n = 7, 11, 15; (II) DCC, HOBt, NMM and Tos·Gly-OBzl; (III) DCC, HOBt, NMM and BocAsp(OBzl)OH; (IV) 2 N NaOH; (V) 4 N HCl−EtOAc; (VI) 5% H_2 (0.02 M Ba) Pd/C.

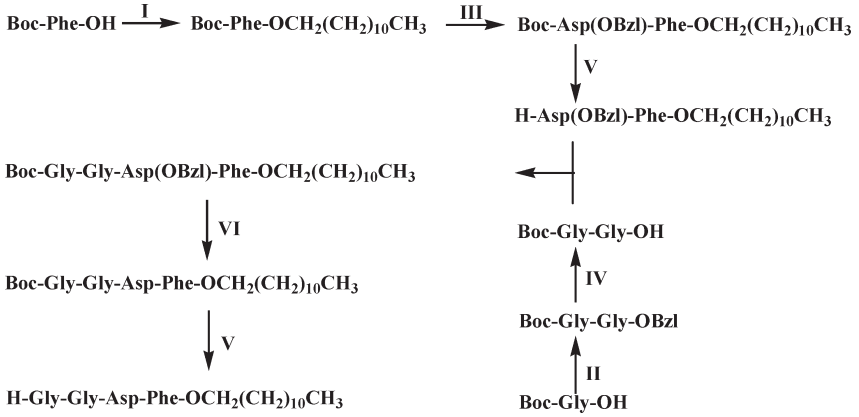

Figure 2. Synthesis of GGDFO$(CH_2)_{11}CH_3$: (I) DCC, HOBt, NMM and $CH_3(CH_2)_{11}OH$; (II) DCC, HOBt, NMM and Tos·Gly-OBzl; (III) DCC, HOBt, NMM and BocAsp(OBzl)OH; (IV) 2 N NaOH; (V) 4 N HCl−EtOAc; (VI) 5% H_2 (0.02 M Ba) Pd/C.

were then subjected to condensation with Boc-R(NO_2)G-OH or Boc-GG-OH in the presence of DCC and HOBt to yield *N*-α-*tert*-butyloxycarbonyl-*N*-γ-nitro-arginyl-glycyl-4-benzylaspartyl-phenylalanyl fatty alcohol esters [Boc-R(NO_2)GD(OBzl)FO$(CH_2)_nCH_3$, n = 7, 11 or 15] (Figure 1) or [Boc-GGD(OBzl)FO$(CH_2)_{11}CH_3$] (Figure 2). Both nitro and benzyl protection groups were removed via catalytic hydrogenation in the presence of Pd/C to yield [Boc-RGDFO$(CH_2)_nCH_3$, n = 7, 11 or 15] (Figure 1) or [Boc-GGDFO$(CH_2)_{11}CH_3$] (Figure 2). Finally the *N*-*tert*-butyloxycarbonyl protection group was removed in 4 N HCl−EtOAc to yield [RGDFO$(CH_2)_nCH_3$, n = 7, 11 or 15] (Figure 1) or [GGDFO$(CH_2)_{11}CH_3$] (Figure 2).

2.3. Preparation of Liposomal Formulations. L-RGDF-DOXs were prepared according to a method reported by others[24,25] with modifications. In brief, phospholipids, cholesterol and RGDFO$(CH_2)_nCH_3$ (n = 7, 11, 15) (molar ratio: 14.25:4.75:1) were dissolved in chloroform in a flask. Chloroform was evaporated under reduced pressure to form a lipid film, which was subsequently mixed with 120 mM ammonium sulfate. The mixture was vortexed. The fully hydrated mixture was sonicated for 10 min to obtain an opaque liposomal preparation, which was sealed in a dialysis bag (molecular weight cutoff: 8,000−14,000 Da) and dialyzed against saline for 8 h. After five times of repeated dialysis, the resultant liposomal preparation was placed in a flask. In a separate flask, doxorubicin hydrochloride (DOX:phospholipids 1:20 w/w) was dissolved in a small quantity of distilled water. The above liposomal preparation and DOX were mixed and shaken at 37 °C in a water bath for 30 min to yield L-RGDF-DOXs. Conventional L-DOX or liposomal DOX preparation without RGDF−fatty alcohol conjugate incorporated was obtained using the same protocol except that RGDFO$(CH_2)_nCH_3$ was not included in the procedure. To study the effect of the amount of RGDF on the anticancer activity and targeting potential in liposomal DOX, a second RGDF−lauryl conjugate incorporated liposomal DOX preparation (L-RGDFC12-DOX) was also obtained using phospholipids, cholesterol and RGDFO$(CH_2)_{11}CH_3$ at a molar ratio of 14.25:4.75:0.5. Using the same protocol, GGDF−lauryl alcohol conjugate incorporated liposomal DOX preparation (L-GGDF-DOX) was also prepared. DOX encapsulation efficiency was determined according to a previously reported method.[26] In brief, 0.5 mL of the respective liposomal preparation was loaded onto a Sephadex G50 column, which was eluted with normal saline solution at a flow rate of 1.5 mL/min to separate free DOX from liposomes. The liposomal fraction or liposomes loaded with DOX were collected and transferred to a 25 mL flask into which 0.1 mL of 10% Triton X-100 was added, and the final volume was adjusted to 25 mL using normal saline. The mixture was

thoroughly mixed to allow DOX that was incorporated into the liposomes to be released, and the amount of DOX released (which is referred to as DOX encapsulated) was determined at 496 nm using a spectrophotometer. In a separate test, 0.5 mL of the respective liposomal preparation was placed in a 25 mL flask, into which 0.1 mL of 10% TritonX-100 was added, and the final volume was adjusted to 25 mL using normal saline. The mixture was mixed thoroughly to allow any DOX that was incorporated into the liposomes to be released. The amount of DOX was determined and considered as total DOX (free DOX and DOX encapsulated). The encapsulation efficiency was calculated as the amount of DOX encapsulated/total DOX. The experiment was repeated three times. The morphology of liposomes was examined by TEM. Particle sizes and zeta-potentials of liposomes were analyzed by a particle size analyzer, Zetasizer Nano ZS-90.

2.4. *In Vitro* Release of DOX from Its L-RGDF-DOXs. The release of DOX from its L-RGDF-DOXs was determined using L-RGDFC12-DOX according to the method reported by Kim et al.[27] Briefly, 2 mL of L-RGDFC12-DOX was placed and sealed in a dialysis bag, which was placed in a beaker containing 50 mL of phosphate buffered saline (PBS, pH 7.4) and dialyzed in a shaker at 37.5 °C. At different time intervals (1, 2, 4, 6, 12, 24, 48, and 72 h), 50 mL of the PBS in the beaker was removed and replaced with 50 mL of fresh PBS to maintain a sink condition. Concentrations of DOX in the PBS withdrawn were analyzed at 496 nm using a spectrophotometer. Total DOX released over the 72 h monitored was calculated, and results were plotted.

2.5. *In Vivo* Anticancer Activities of L-RGDF-DOXs in Mice Inoculated with S_{180} Sarcoma. The anticancer activity was determined in ICR mice (Swiss) inoculated with S_{180} sarcoma. Mice were maintained in accordance with institutional guidelines. S_{180} tumor cells passaged in Kunming mice abdomen were harvested on the eighth day and suspended in saline at 2.0×10^7/mL, which was injected to ICR mice (0.2 mL/per mouse). The mice inoculated with S_{180} tumor cells were randomly divided into 12 different groups with 10 in each group. Twenty-four hours after inoculation (day 1), mice were injected (0.2 mL/animal) with 2 mg/kg of DOX in doxorubicin hydrochloride solution (S-DOX), L-DOX, L-RGDFC12-DOX, RGDF−capryl alcohol conjugate incorporated liposomal DOX (L-RGDFC8-DOX) or RGDF−cetyl alcohol conjugate incorporated liposomal DOX (L-RGDFC16-DOX) via the tail vein, and injection was repeated on days 4 and 7. Two days after the final injection, mice were sacrificed and tumors were weighed. Blank liposomal preparation with no RGDFO$(CH_2)_nCH_3$ or DOX (L) and saline (NS) were used as negative controls. Furthermore, L-GGDFC12-DOX (2 mg/kg of DOX) was also used as a control. To study the effect of the concentration of RGDF in the liposomal preparations on anticancer activity, 2 mg/kg of DOX in L-RGDFC12-DOX prepared using different amounts of RGDFC12 as described in section 2.3 was injected to mice inoculated with S_{180} tumor cells. The anticancer activities of L-RGDF-DOXs given with different dosages of DOX (1 mg/kg, 2 mg/kg and 3 mg/kg) were also studied. Data are expressed as $X \pm$ SD, and statistical significance was determined using unpaired two-sided Student's *t*-test. Removed tumor tissues were washed with saline, wrapped with tinfoil and stored at −80 °C for subsequent tissue dissection and hematoxylin−eosin staining. Sliced tissues were examined and photographed under a microscope.

2.6. Biodistribution of S-DOX, L-GGDFC12-DOX and L-RGDFC12-DOX in Tumor Bearing Mice. Tissue distribution of L-RGDF-DOXs was determined according to a method reported by others.[9] In brief, S_{180} tumor cells passaged in the abdomens of the Kunming mice were harvested on the eighth day and suspended at 2.0×10^7/mL. The tumor cell preparation ($\sim 2 \times 10^6$ tumor cells) was injected subcutaneously under the right armpit of each of the 120 ICR mice (22−24 g). Seven days later, mice were randomly divided into three different groups with 40 in each group which were injected via the tail vein with 7.5 mg/kg of DOX in S-DOX, L-GGDFC12-DOX or L-RGDFC12-DOX (40 mice for each preparation). At each time interval (5 min, 15 min, 30 min, 1 h, 4 h, 8 h, 24 h and 48 h) after injection of the respective formulations, blood samples from five mice were collected, and mice were then sacrificed. Both the heart and tumor were removed, washed with distilled water, dried with paper towel, weighed and frozen at −20 °C. Heart and tumor tissues were homogenized with PBS (1 g of tissue:3 mL of PBS), and homogenized tissue samples were transferred to centrifuge tubes. To each centrifuge tube, 50 μL of methanol and 50 μL of daunorubicin (1 μg/mL) as an internal standard were added and vortexed. The homogenates were subjected to extraction using chloroform and methanol (4:1) (3 mL for tumor and 1.5 mL for heart). The tubes were vortexed for 3 min and centrifuged at 1000*g* for 10 min. An aliquot of the organic layer was removed and dried. The residue was dissolved in 180 μL of HPLC grade methanol, and the solution was analyzed by HPLC (21) using a C-18 column and acetonitrile:water (30:70)[28,29] as mobile phase at 0.8 mL/min with UV detection at $\lambda_{max} = 254$ nm. DOX concentrations versus time were plotted.

According to the method proposed by Hunt et al.,[30] the following calculations were carried out to obtain therapeutic availability (TA) and drug targeting index (DTI):

$$TA = AUC_{targetDC}/AUC_{targetD}$$

$$DTI = (AUC_{targetDC}/AUC_{toxDC})/(AUC_{targetD}/AUC_{toxD})$$

where "target" represents the targeted site, which is the tumor in this study, "tox" represents the major toxic organ/tissue, which is the heart in this study,[4−6] "DC" represents the site specific formulations being studied, which are L-RGDF-DOX preparations, and "D" represents the same amount of free drug or negative controls used, which are conventional L-DOX and L-GGDFC12-DOX. When TA is >1, the site specific formulations studied are considered having targeting capability.

3. RESULTS AND DISCUSSION

To synthesize RGDFO$(CH_2)_nCH_3$ (n = 7, 11 and 15) and GGDFO$(CH_2)_{11}CH_3$, the N-termini of the respective peptides were protected with $(Boc)_2O$ and C-termini were protected with benzyl esters. In most of the condensation procedures where peptide amide bonds were formed, excess amounts of DCC were added. The esterification of the respective fatty alcohols to phenylalanine was found to be slow and incomplete, and excess amounts of fatty alcohols were used. Because of the difficulty in removing unreacted fatty alcohols, the ratio of fatty alcohol to phenylalanine was kept at not more than 1.5. The products, RGDFO$(CH_2)_nCH_3$ (n = 7, 11 or 15) and GGDFO-$(CH_2)_{11}CH_3$, were purified using silica gel columns eluted with gradient chloroform and methanol (120:1, 100:1, 90:1 and 80:1). The purities of compounds were found to be more than 90% as determined by HPLC. Purified compounds were characterized using ^1H and ^{13}C nuclear magnetic resonance (NMR) and mass spectrometry (MS). Melting points and specific optical rotation

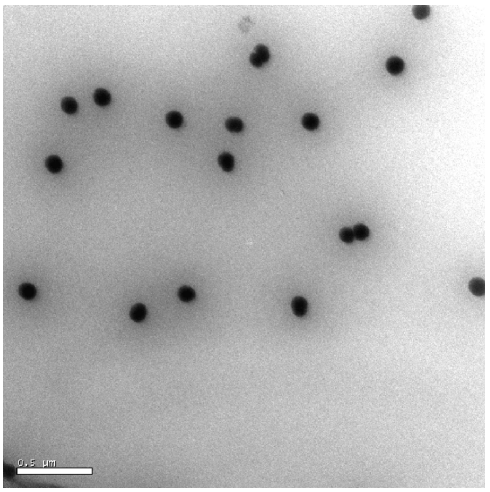

Figure 3. TEM photograph of L-RGDFC12-DOX showing spherical shaped particles.

Table 1. Particle Sizes and Zeta Potentials of Various DOX Liposomes

formulation	particle size (nm)	zeta potential (mV)
L-RGDFC8	233.0 ± 1.1	−44.80 ± 0.66
L	191.0 ± 2.4	−46.33 ± 2.51
L-DOX	227.6 ± 7.4	−41.78 ± 1.32
L-RGDFC8-DOX	143.9 ± 0.6	−52.30 ± 1.76
L-RGDFC12-DOX	244.0 ± 2.9	−48.76 ± 3.72
L-RGDFC16- DOX	176.5 ± 1.4	−43.15 ± 2.04
L-GGDFC12-DOX	216.0 ± 7.8	−59.79 ± 1.33
2.5% L-RGDFC8-DOX	248.5 ± 1.2	−44.73 ± 2.43
L-RGDFC8-DOX 1 mg	250.2 ± 7.2	−43.63 ± 2.49
L-RGDFC8-DOX 3 mg	223.9 ± 9.9	−49.70 ± 1.64

of the purified final products were also determined. Detailed chemistry data of the four peptide fatty alcohol conjugates are provided in the Supporting Information.

Because of the amphipathic nature of RGDF− or GGDF−fatty alcohol conjugates, they are expected to be readily incorporated into liposomes. The fatty alkanyl chains are likely to be intercalated between fatty acyl chains of liposomal bilayers while the hydrophilic peptide moiety (RGDF or GGDF) is likely to be anchored on the surface of liposomes and projected to an aqueous environment.

DOX was loaded into liposomes including RGDF−fatty alcohol conjugate incorporated, GGDF−lauryl alcohol conjugate incorporated and conventional liposome using a transmembrane pH gradient method as described above. The morphology of the RGDF−fatty alcohol conjugate incorporated liposomal DOX preparations was studied, and results of L-RGDFC12-DOX are shown in Figure 3 as an example. Under the TEM, the liposomal DOX preparations were found to exist as spherical particles with an average size of ∼200 nm. The particle size and zeta-potential of the liposomal formulations prepared were examined, and the results are summarized in Table 1. It was found that the particle sizes of most formulations were between 190 and 250 nm, and the zeta-potentials were found to be about −45 mV. It should be noted that RGDF is electronically neutral as it contains one acidic (D), one basic (R) and 2 neutral (G and F) amino acids. Given the molar ratio of phospholipids to RGDF in RGDF incorporated liposomal preparations being 14.25:1 (or 14.25:0.5), the zeta potential of RGDF incorporated liposomal preparations reflected the charge of phospholipids found in the liposomes. Although GGDF possesses a negative charge, the zeta potential of GGDF incorporated liposomal preparation is primarily determined by the charge of the phospholipids since the amount of GGDF in the GGDF incorporated liposomal preparation was very small in comparison to that of phospholipids (1:14.25). The encapsulation efficiency of DOX into liposomes was about 94%.

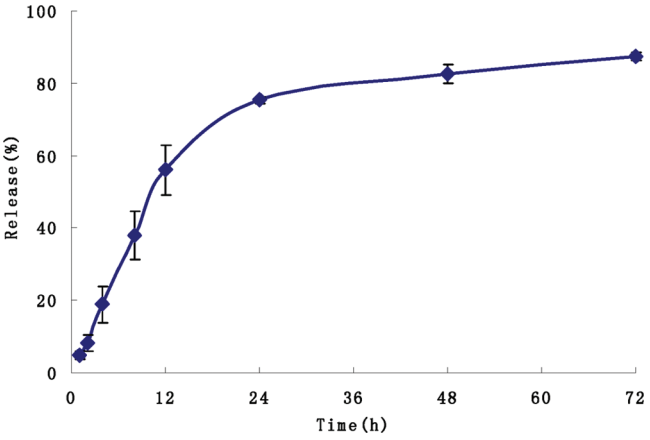

Figure 4. *In vitro* release of DOX from L-RGDFC12-DOX ($N = 3$).

The release of DOX from L-RGDF-DOX preparations over time was studied using L-RGDFC12-DOX, and it was found that DOX was slowly released as shown in Figure 4. About 60% of encapsulated DOX was released within the first 12 h. At 72 h, almost 90% of encapsulated DOX was released.

The antitumor activities of L-RGDF-DOXs were evaluated in ICR mice inoculated with S_{180} sarcoma. Tumor weights were determined and compared among mice administered with various preparations. As shown in Figure 5, all liposomal DOX preparations were found to have improved effect in reducing tumor growth in comparison with S-DOX. There was little difference between L-DOX and L-GGDFC12-DOX, suggesting that GGDF had little effect on the anticancer activity of liposomal DOX preparation. However, L-RGDF-DOXs were found to be more effective than L-DOX and L-GGDFC12-DOX. The results suggest that RGDF might have delivered more DOX to tumor cells due to its affinity for the integrins overexpressed in tumor cells. There was no significant difference found among the various RGDF−fatty alcohol conjugates studied.

To further examine the targeting potential of RGDF, three different doses of DOX (1, 2, and 3 mg/kg) in L-RDGFC12-DOX were administered to tumor-bearing mice, and results are shown in Figure 6. It was found that there was little difference between 2 and 3 mg/kg of DOX although the effect of 1 mg/kg of DOX was found to be significantly lower. By comparing the results in Figures 5 and 6, it was found that the tumor size following 1 mg/kg of DOX in L-RGDFC12-DOX formulation was similar to that of 2 mg/kg of DOX in L-DOX, suggesting that RGDF incorporated liposomal DOX was able to achieve the same effect as higher L-DOX perhaps by directing more DOX to tumor sites.

The effect of the amount of RGDF−lauryl alcohol conjugate in liposomal DOX on tumor size was also examined with

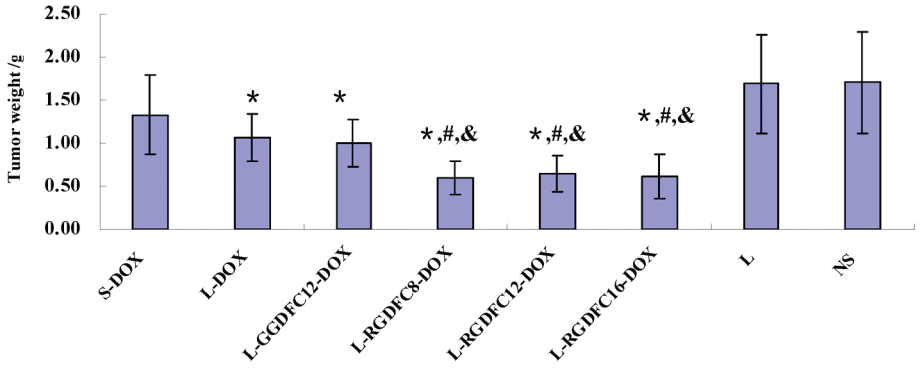

Figure 5. Tumor weights in mice inoculated with S_{180} following tail vein injection of 2 mg/kg of L-RGDF-DOXs on days 1, 4, and 7 (N = 10). *Significant compared to S-DOX (P > 0.05). #Significant compared to liposomal DOX preparation or L-DOX (P > 0.01). &Significant compared to L-GGDFC12-DOX (P > 0.01).

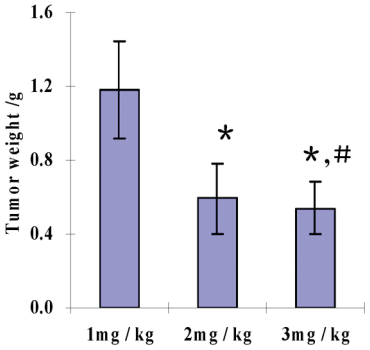

Figure 6. Tumor weights in tumor-bearing mice administered with L-RGDFC12-DOX preparations containing 1, 2, and 3 mg/kg of DOX (N = 10). *Significant compared to 1 mg/kg of DOX (P > 0.01). #Insignificant compared to 2 mg/kg of DOX (P > 0.05).

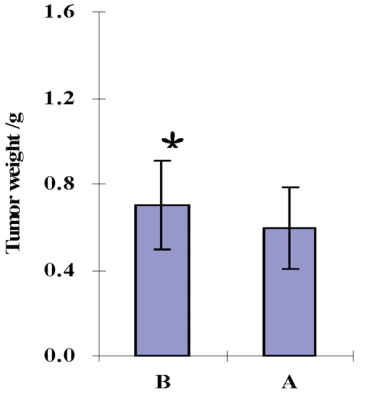

Figure 7. Tumor weights in mice inoculated with S_{180} sarcoma following tail vein injection of two L-RGDFC12-DOX preparations, A and B (N = 10). *Insignificant compared to 5.0% (P > 0.05). A: prepared with phospholipids, cholesterol and RGDFO$(CH_2)_{11}CH_3$ at a molar ratio of 14.25:4.75:0.5. B: prepared with phospholipids, cholesterol and RGDFO$(CH_2)_{11}CH_3$ at a molar ratio of 14.25:4.75:1.

L-RGDFC12-DOX containing two different amounts of RGDF, one prepared with phospholipids, cholesterol and RGDFO-$(CH_2)_{11}CH_3$ at a molar ratio of 14.25:4.75:1 and the other with phospholipids, cholesterol and RGDFO$(CH_2)_{11}CH_3$ at 14.25:4.75:0.5. Both preparations were administered to mice inoculated with S_{180} sarcoma, and tumor size was determined as described above. As shown in Figure 7, there was little difference between the two L-RGDFC12-DOX preparations studied, which suggested that the number of receptors on the surface of tumor cells is limited and the cellular uptake is saturable.

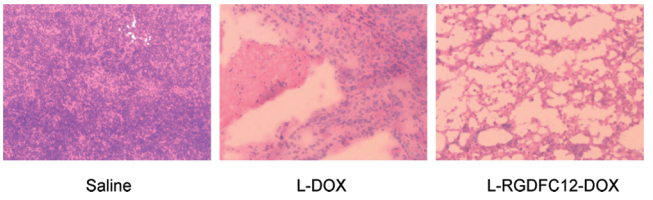

Figure 8. Tumor biopsy (H&E staining, 10 × 10 magnification) after tail vein injection of saline, 2 mg/kg of DOX in L-DOX and L-RGDFC12-DOX in S_{180} inoculated mice.

In addition to tumor size, pathological examination is also important in assessing the antitumor potential of cytotoxic agents. Figure 8 shows the H&E stained images of tumor tissues dissected from ICR mice inoculated with S_{180} after treatment with different DOX formulations. The left panel in Figure 8 is tumor cells treated with saline in which nuclei of tumor cells were clearly stained indicating viable tumor cells. Following the treatment of L-DOX (middle panel), localized tumor cell death and cytolysis were observed. However, there were still a significant number of unlysed tumor cells with intact nuclei shown. Treatment with L-GGDFC12-DOX resulted in an image similar to that with L-DOX (image not shown). Following the treatment of L-RGDFC12-DOX (right panel), more dead tumor cells were observed and the structure of tumor tissues was significantly damaged.

The results of pathological examinations were consistent with those of tumor size. Compared to L-DOX, L-RGDFC12-DOX was shown to be more effective, suggesting that elevated concentrations of DOX may have been delivered to the tumor site via RGDF moiety.

The pharmacokinetic profiles and tissue distribution of S-DOX, L-GGDFC12-DOX and L-RGDFC12-DOX were studied. Concentrations of DOX in plasma, tumor and heart at different time intervals after tail vein injection of DOX formulations were determined using HPLC. Figure 9 shows plasma concentrations of DOX following administration of S-DOX, L-GGDFC12-DOX and L-RGDFC12-DOX. A pharmacokinetic software, 3P87, was used to calculate pharmacokinetic parameters as listed in Table 2.

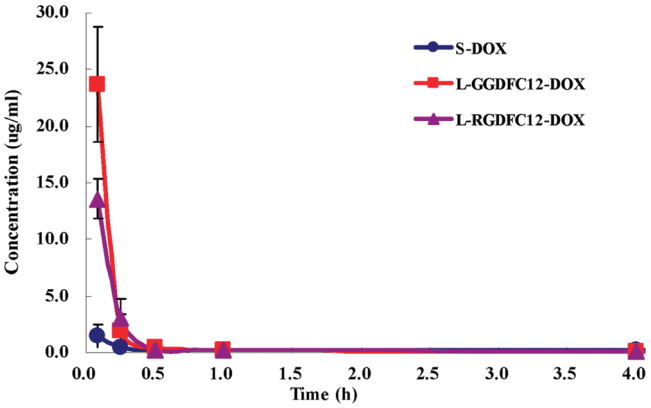

Figure 9. DOX concentrations in plasma in mice inoculated with S_{180} sarcoma following tail vein injection of 7.5 mg/kg of DOX in S-DOX, L-GGDFC12-DOX and L-RGDFC12-DOX ($N = 5$).

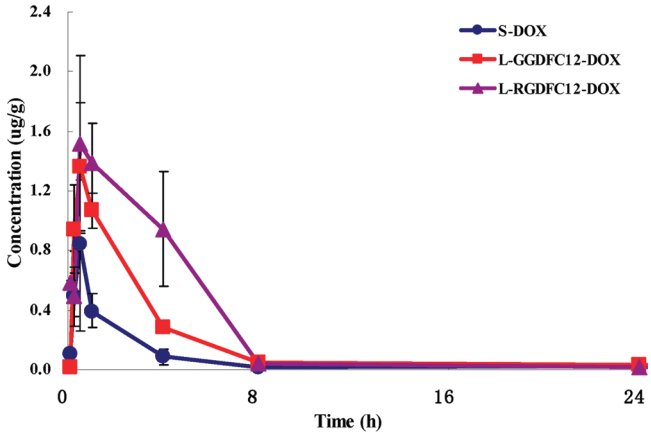

Figure 10. DOX concentrations in the tumor following tail vein injection of S-DOX, L-GGDFC12-DOX and L-RGDFC12-DOX ($N = 5$).

Table 2. Pharmacokinetic Parameters of DOX in Plasma Following Tail Vein Administration of 7.5 mg/kg of DOX in S-DOX, L-GGDFC12- DOX and L-RGDFC12- DOX

parameter	unit	S-DOX	L-GGDFC12-DOX	L-RGDFC12-DOX
A	μg/mL	2.7131	0.3812	37.5397
$V/F(c)$	(mg/kg)/(μg/mL)	2.6046	14.368	0.1989
AUC	(μg/mL)h	38.5630	207.537	86.8256
CL	mg/kg/h/(μg/mL)	0.1944	0.03614	0.08638

Table 3. Pharmacokinetic Parameters in the Tumor Following Tail Vein Injection of DOX, L-GGDFC12-DOX and L-RGDFC12- DOX

parameter	unit	S-DOX	L-GGDFC12-DOX	L-RGDFC12-DOX
A	μg/mL	3.0002	1.6657	0.04121
$V/F(c)$	(mg/kg)/(μg/mL)	5.2873	4.4412	3.1166
AUC	(μg/mL)h	1.6435	3.6514	7.5412
CL	mg/kg/h/(μg/mL)	4.5635	2.0540	0.9945

As shown in Table 2, the area under the curve (AUC) following L-RGDFC12-DOX was 2.25-fold of that following S-DOX while the clearance rate (CL) of L-RGDFC12-DOX was 44% of that of S-DOX. The results indicated that L-RGDFC12-DOX is associated with a reduced plasma clearance or increased circulation time of DOX in comparison to S-DOX. This observation is consistent with the results observed in the *in vitro* release study (Figure 4), which showed a gradual release of DOX from L-RGDFC12-DOX.

To evaluate the targeting capability of RGDF peptide, a tetrapeptide with a sequence of GGRF was designed as a nontargeting moiety or control. By comparison, it was observed that $AUC_{L\text{-}RGDFC12\text{-}DOX}$ was about 42% of $AUC_{L\text{-}GGDFC12\text{-}DOX}$ while the plasma clearance of L-RGDFC12-DOX ($CL_{L\text{-}RGDFC12\text{-}DOX}$) was 2.39-fold of that of L-GGDFC12-DOX ($CL_{L\text{-}GGDFC12\text{-}DOX}$), suggesting that nontargeted peptide incorporated liposomes have a longer circulation time in plasma than RGDF incorporated liposomes (L-RGDFC12-DOX). The RGDF−fatty alcohol conjugate anchored on the surface of liposomes is likely responsible for the reduced circulation time as it may have rapidly directed liposomal DOX to tumor sites and consequently its residence time in plasma was reduced.

Figure 10 shows the concentrations of DOX found in the tumor after tail vein injection of three formulations. The calculated pharmacokinetic parameters of three formulations in tumor tissues are shown in Table 3, which demonstrated that the AUC following RGDF incorporated liposomes ($AUC_{L\text{-}RGDFC12\text{-}DOX}$) was 4.59- and 2.25-fold of that of nontargeted peptide (GGDF) incorporated liposomes ($AUC_{L\text{-}GGDFC12\text{-}DOX}$) and doxorubicin hydrochloride solution ($AUC_{S\text{-}DOX}$), respectively. The maximum concentration of DOX in the tumor observed after the administration of RGDF incorporated liposomes ($C(max)_{L\text{-}RGDFC12\text{-}DOX}$) was 2.4- and 1.3-fold of that of doxorubicin hydrochloride solution ($C(max)_{S\text{-}DOX}$) and nontargeted peptide incorporated liposomes ($C(max)_{L\text{-}GGDFC12\text{-}DOX}$), respectively. The clearance rate of L-RGDFC12-DOX ($CL_{L\text{-}RGDFC12\text{-}DOX}$) in tumor tissues was 22% and 48% of that of doxorubicin hydrochloride solution ($CL_{S\text{-}DOX}$) and nontargeted peptide incorporated liposomes ($CL_{L\text{-}GGDFC12\text{-}DOX}$). The results indicated that the RGDF incorporated liposomal DOX (L-RGDFC12-DOX) resulted in elevated concentrations of DOX in the tumor and reduced clearance of DOX from the tumor in comparison to both doxorubicin hydrochloride solution (S-DOX) and nontargeted peptide incorporated liposomes (L-GGDFC12-DOX). The higher concentration and longer residence time in the tumor are likely responsible for the improved antitumor activities observed as shown in Figures 5 and 8.

A very important mechanism of doxorubicin cardiotoxicity involves the formation of cytotoxic free radicals such as superoxide radical anion and hydroxyl radical, both of which are formed via reduction of the anthracyclinone quinine to hydroquinone by NADPH/CYP450 reductase. The production of hydroxyl radicals inside tumor cell might augment the antineoplastic effect of the anthracyclines, but such formation is uncommon at standard antineoplastic doses.[4] Cytotoxic radicals generated in the heart are believed to be responsible for acute and often severe cardiotoxicity. Cardiac tissue is vulnerable to the attack of free radicals because it lacks the catalase enzyme,[4,6] which converts hydrogen peroxide to harmless water and oxygen. The hydrogen peroxide generated in the myocardium will eventually become highly reactive hydroxyl radicals. In addition, the active secondary C_{13}- alcohol metabolites of anthracycline

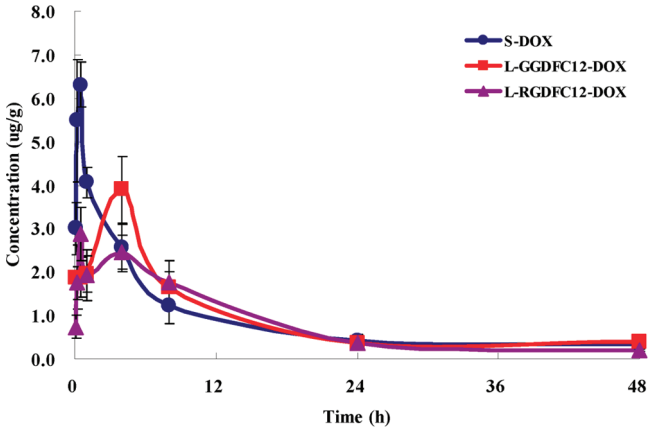

Figure 11. DOX concentrations in the heart following tail vein injection of S-DOX, L-GGDFC12-DOX and L-RGDFC12-DOX ($N = 5$).

Table 4. Pharmacokinetic Parameters of DOX in the Heart Following Tail Vein Administration of 7.5 mg/kg of DOX in S-DOX, L-GGDFC12- DOX and L-RGDFC12- DOX

parameter	unit	S-DOX	L-GGDFC12-DOX	L-RGDFC12-DOX
A	μg/mL	4.993	2.0137	2.3632
$V/F(c)$	(mg/kg)/(μg/mL)	1.5020	3.7244	3.1737
AUC	(μg/mL)h	32.1275	60.7558	50.4140
CL	mg/kg/h/(μg/mL)	0.2334	0.1488	0.1234

Table 5. Targeting Parameters of L-RGDFC12-DOX in Mice Inoculated with S_{180} Sarcoma

	TA	DTI
compared with S-DOX	4.59	2.43
compared with L-GGDFC12-DOX	2.07	1.71

anticancer agents can also lead to chronic cardiomyopathy. For example, C_{13}-hydroxyl doxorubicin (doxirubicinol) formed induces a prolonged inhibition of calcium loading, opens selective ion channels leading to increased cytosolic levels of Ca^{2+} in the sarcoplasmic reticulum, and inhibits Na^+/K^+-ATPase action in the sarcolemma. These important cellular events can induce a chronic cardiomyopathy that presents a severe congestive heart failure.[5] In the current study RGDF was designed to direct more DOX in liposomes to tumor cells and reduce the DOX accumulation in the heart. Figure 11 shows the concentrations of DOX found in the heart after tail vein injection of RGDF incorporated liposomal DOX in comparison to DOX solution and GGDF incorporated liposomal DOX. The calculated pharmacokinetic parameters of the three formulations in the heart are shown in Table 4, and the concentrations of DOX in the heart are represented in Figure 11. DOX from S-DOX reached its peak concentration within minutes, and the peak concentration was much higher than that after liposomal formulations (L-GGDFC12-DOX and L-RGDFC12-DOX). The liposomal preparations reached their peak concentrations in about 4 h after tail vein administration. It was also found that the cardiac concentration of DOX following the administration of L-RGDFC12-DOX was the lowest in comparison to S-DOX and L-GGDFC12-DOX. The results indicated that liposomal formulations of DOX significantly reduced DOX accumulation in the heart in comparison to free DOX solution. Compared to GGDF incorporated liposomes, RGDF incorporated liposomes (L-RDGFC12-DOX) diverted more DOX to tumor tissues and reduced accumulation of DOX in the heart.

The targeting potential of L-RGDFC12-DOX in comparison to S-DOX and L-GGDFC12-DOX was determined according to the method proposed by Hunt and his research group,[30] and targeting parameters including TA and DTI were calculated. The results are summarized in Table 5

The TA values of L-RGDFC12-DOX in comparison to S-DOX and L-GGDFC12-DOX are 4.59 and 2.07, respectively, indicating the targeting capacity of RGDF for tumor site. The DTI values of L-RGDFC12-DOX in comparison to S-DOX and L-GGDFC12-DOX are 2.43 and 1.71, respectively, again indicating the targeting capacity of RGDF.

Liposomal DOX formulations have been studied by several research groups.[31,32] In most studies, the dosage of DOX needed to exhibit significant inhibition of tumor growth was 5 mg/kg. In this study, a dose of 2 mg/kg of DOX in RGDF incorporated liposomal preparations was shown to have a significant effect on tumor growth, suggesting that RGDF improved the efficacy of liposomal DOX, which is likely a result of more DOX molecules delivered to tumor sites when RGDF was incorporated in the liposomal preparation. The results supported the hypothesis that RGDF, as a tumor specific peptide, can direct the delivery of liposomal DOX to tumors.

In conclusion, RGDF modified DOX liposomal preparation achieved much improved delivery to tumors while levels of DOX to the heart were significantly reduced in comparison to conventional liposomal preparations.

■ ASSOCIATED CONTENT

Supporting Information. Detailed chemistry data of the four peptide fatty alcohol conjugates. This material is available free of charge via the Internet at http://pubs.acs.org.

■ AUTHOR INFORMATION

Corresponding Author

*H.L.: Memorial University of Newfoundland, School of Pharmacy, 300 Prince Philip Drive, St. John's, Newfoundland, Canada A1B 3V6; tel, +1 709 777 6382; fax, +1 709 777 7044; e-mail, hliu@mun.ca. G.C.: tel, +86 010 83911538; fax, +86 10 8391 1533; e-mail, cuiguohui@bjmu.edu.cn or cgh@ccmu.edu.cn. G.C.: School of Chemical Biology and Pharmaceutical Sciences, Capital Medical University, Beijing, China. 100069.

Author Contributions

‡Authors who contributed equally to the study.

■ ACKNOWLEDGMENT

This research was supported by the National Natural Science Foundation of China (30873202). The authors are also grateful to the Key Laboratory on Peptides and Small Drug Molecules and the Modern Drug Analysis Laboratory at the Capital Medical University for their generous help.

REFERENCES

(1) Fornari, F. A.; Randolph, J. K.; Yalowich, J. C.; Ritke, M. K.; Gewirtz, D. A. Interference by doxorubicin with DNA unwinding in MCF-7 breast tumor cells. *Mol. Pharmacol.* **1994**, *45*, 649–656.

(2) Gerwirtz, D. A. A critical evaluation of the mechanisms of action proposed for the antitumor effects of the anthracycline antibiotics adriamycin and daunorubicin. *Biochem. Pharmacol.* **2001**, *57*, 727–741.

(3) Mayo Clinic, Doxorubicin (Systemic) 2007. http://web.archive.org/web/20070403223644/http://www.mayoclinic.com/health/drug-information/DR202209.

(4) Kwok, J. C.; Richardson, D. R. Examination of the mechanism(s) involved in doxorubicin-mediated iron accumulation in ferritin: studies using metabolic inhibitors, protein synthesis inhibitors and lysosomotropic agents. *Mol. Pharmacol.* **2004**, *65*, 181–195.

(5) Lothstein, L.; Isreal, M.; Sweatman, T. W. Anthracycline drug targeting: cytoplasmic versus nuclear—a fork in the road. *Drug Resist. Updates* **2001**, *4* (3), 169–177.

(6) Swain, S. M.; Vici, P. The current and future role of dexrazoxane as a cardioprotectant in anthracycline treatment: expert panel review. *J. Cancer Res. Clin. Oncol.* **2004**, *130*, 1–7.

(7) Ogawara, K.; Un, K.; Minato, K.; Tanaka, K.; Higaki, K.; Kimura, T. Determinants for in vivo anti-tumor effects of PEG liposomal doxorubicin: Importance of vascular permeability within tumor. *Int. J. Pharm.* **2008**, *359*, 234–240.

(8) Yang, T.; Choi, M. K.; Cui, F.; Kim, J. S.; Chung, S. J.; Shim, C. K.; Kim, D. D. Preparation and evaluation of paclitaxel-loaded PEGylated immunoliposome. *J. Controlled Release* **2007**, *120*, 169–177.

(9) Pan, H.; Han, L.; Chen, W.; Yao, M.; Lu, W. Targeting to tumor necrotic regions with biotinylated antibody and streptavidin modified liposomes. *J. Controlled Release* **2008**, *125*, 228–235.

(10) Saul, J. M.; Annapragada, A.; Natarajan, J. V.; Bellamkonda, R. V. Controlled targeting of liposomal doxorubicin via the folate receptor in vitro. *J. Controlled Release* **2003**, *92*, 49–67.

(11) Yeh, C. H.; Peng, H. C.; Huang, T. F. Accutin, a new disintegrin, inhibits angiogenesis in vitro and in vivo by acting as integrin alphavbeta3 antagonist and inducing apoptosis. *Blood* **1998**, *92*, 268–3276.

(12) Schmitmeier, S.; Markland, F. S.; Chen, T. C. Anti-invasive effect of contortrostatin, a snake venom disintegrin, and TNF-alpha on malignantglioma cells. *Anticancer Res.* **2000**, *20*, 4227–4233.

(13) Humphries, M. J. Integrin structure. *Biochem. Soc. Trans.* **2004**, *28*, 311–339.

(14) Hynes, R. O. Integrins: versatility, modulation, and signalingin cell adhesion. *Cell* **1992**, *69*, 11–25.

(15) Tucker, G. C. Inhibitors of intergrins. *Curr. Opin. Pharmacol.* **2002**, *2*, 394–402.

(16) Alford, D.; Pitha-Rowe, P.; Taylor-Papadimitriou, J. Adlhesion molecules in breast cancer: role of $\alpha_2\beta_1$ integrin. *Biochem. Soc. Symp.* **1998**, *63*, 245–259.

(17) Johnson, J. P. Cell adhesion molecules in the development and progression of malignant melanoma. *Cancer Metastasis Rev.* **1999**, *18*, 345–357.

(18) Max, R.; Gerritsen, R. R.; Nooijen, P. T. Immunohistochemical analysis of integrin $\alpha_V\beta_3$ expression on tumor-associated vessels of human carcinomas. *Int. J. Cancer* **1997**, *71*, 320–324.

(19) Strömblad, S.; Cheresh, D. A. Integrins, angiogenesis and vascular cell survival. *Chem. Biol.* **1996**, *3*, 881–885.

(20) Xiong, X.; Huang, Y.; Lu, W.; Zhang, X.; Zhang, H.; Zhang, Q. Preparation of doxorubicin in loaded stealth liposomes modified with RGD mimetic and cellular association in vitro. *Acta Pharmacol. Sin.* **2005**, *40*, 1085–1090.

(21) Jain, S.; Mishra, V.; Singh, P.; Dubey, P. K.; Saraf, D. K.; Vyas, S. P. RGD-anchored magnetic liposomes for monocytes/neutrophils-mediated brain targeting. *Int. J. Pharm.* **2003**, *261*, 43–55.

(22) Rahman, S.; Lu, X.; Kakkar, V. V.; Authi, K. S. The integrin $\alpha_{IIb}\beta_3$ contains distinct and interacting binding sites for snake-venom R-G-D (Arg-Gly-Asp) proteins. *Biochem. J.* **1995**, *312*, 223–232.

(23) Lee, K. H.; Jung, K. H.; Song, S. H.; Kim, D. H.; Lee, B. C.; Sung, H. J.; Han, Y. M.; Choe, Y. S.; Chi, D. Y.; Kim, B. T. Radiolabeled RGD uptake and α_V integrin expression is enhanced in ischemic murine hindlimbs. *J. Nucl. Med.* **2005**, *46*, 472–478.

(24) Han, H. D.; Lee, A.; Hwang, T.; Song, C. K.; Seong, H.; Hyun, J.; Shin, B. C. Enhanced circulation time and antitumor activity of doxorubicin by comb-like polymer-incorporated liposomes. *J. Controlled Release* **2007**, *120*, 161–168.

(25) Haran, G.; Cohen, R.; Bar, L. K.; Barenholz, Y. Transmembrane ammonium sulfate gradient in liposomes produce efficient and stable entrapment of amphipathic weak bases. *Biochim. Biophys. Acta* **1993**, *1151*, 201–215.

(26) Shiraga, E.; Barichello, J. M.; Ishida, T.; Kiwada, H. A metronomic schedule of cyclophosphamide combined with PEGylated liposomal doxorubicin has a highly antitumor effect in an experimental pulmonary metastatic mouse model. *Int. J. Pharm.* **2008**, *353*, 65–73.

(27) Yang, S. R.; Lee, H. J.; Kim, J.-D. Histidine-conjugated poly(amino acid) derivatives for the novel endosomolytic delivery carrier of doxorubicin. *J. Controlled Release* **2006**, *114*, 60–68.

(28) Wang, J.-C.; Liu, X.-Y.; Lu, W.-L.; Chang, A.; Zhang, Q.; Goh, B.-C.; Lee, H.-S. Pharmacokinetics of intravenously administered stealth liposomal doxorubicin modulated with verapamil in rats. *Eur. J. Pharm. Biopharm.* **2006**, *62*, 44–51.

(29) Missirlis, D.; Kawamura, R.; Tirelli, N.; Hubbell, J. A. Doxorubicin encapsulation and diffusional release from stable, polymeric, hydrogel nanoparticles. *Eur. J. Pharm. Sci.* **2006**, *29*, 120–129.

(30) Hunt, C. A.; MacGregor, R. D.; Siegel, R. A. Engineering Targeted *In Vivo* Drug Delivery I. The Physiological and Physicochemical Principles Governing Opportunities and Limitations. *Pharm. Res.* **1986**, *3*, 333–344.

(31) Drummond, D. C.; Meyer, O.; Hong, K.; Kirpotin, D. B.; Papahadjopoulos, D. Optimizing liposomes for delivery of chemotherapeutic agents to solid tumors. *Pharmcol. Rev.* **1999**, *51*, 691–743.

(32) Soloman, R.; Gabizon, A. Clinical pharmacology of liposomal anthracyclines: focus on pegylated liposomal Doxorubicin. *Clin. Lymphoma Myeloma* **2008**, *8*, 21–32.